

Anodic oxidation of synthetic refinery effluent on lead anode: mass transport and charge rate balance

T. Zier ^{*}, S. Bouafia-Chergui and M. Chabani

Laboratoire Génie de la Réaction, Equipe procédés durables de dépollution, Faculté de Génie des Procédés et Génie Mécanique, U.S.T.H.B., BP 32, El Allia, Bab Ezzouar, Algeria

^{*}Corresponding author. E-mail: tzier@usthb.dz

 TZ, 0000-0002-4718-7955

ABSTRACT

A synthetic wastewater based on Algiers refinery real effluent was prepared and treated using anodic oxidation. Full factorial plan design was used to conduct the statistical analysis of the results. The aim of the study was to assess the interaction between current density (CD) and stirring degree (SD), and quantify their effects on chemical oxygen demand (COD) removal and electric energy specific consumption (EESC). With an initial COD of 487 mg/L, pH of 5.5 and 0.05 M of Na₂SO₄ as supporting electrolyte, it was found that a 55 rpm stirring degree variation led to a substantial gain in COD removal and energy consumption: 6% and 8.5 kWh/kg, respectively. Current density was found to have a different effect on removal efficiency within the applied stirring domain, and mass transport coefficient (*km*) is inversely correlated to energy consumption. A theoretical model describing the process was reviewed and the relation between concentration, hydrodynamics and applied current was emphasized.

Key words: anodic oxidation, mass transfer, petroleum refinery effluent, wastewater treatment

HIGHLIGHTS

- A simple empirical modeling to assess charge rate and mass transport rate balance (i.e. operating regime).
- Lead anode was first applied for electro-oxidation of toluene.
- Perspectives on the up-scaling approach taken and comparative data were discussed.
- Theoretical modeling review.

INTRODUCTION

Fresh water quality and availability is a major concern worldwide; the increasing demand of this valuable resource is significant in the last years, due to human demographic and industrial growth. It is estimated that more than 40% of the global population will face water stress or scarcity within the next decades (Bartolomeu *et al.* 2018). In response to the increasing demand for energy and petrochemicals, where oil will account for the major world needs in the next decades, a huge amount of water is consumed by the oil processing industry. Refineries' liquid effluents are complex matrices of organic and inorganic pollutants; the quantitative and qualitative contamination depends on the unit configuration and the crude oil nature. The major pollutants found in the effluent are oil and greases, which are the source for other hazardous compounds such as phenols, BTEX, naphthenic acids (NA) and poly-aromatic hydrocarbons (PAH) (Fakhru'l-Razi *et al.* 2009; Aljuboury *et al.* 2017; Ali *et al.* 2018; Al-Khalid & El-Naas 2018; Singh & Shikha 2019).

Electrochemical treatment pathways have gained attention due to the possibility of treating a wide range of organic substances (Yan *et al.* 2014; García-Espinoza & Nacheva 2019). The main advantage to electrochemical treatment is the capability to convert pollutants into CO₂ and water, rather than creating concentrated waste streams. However, this technique still suffers from high-energy consumption and production of critical intermediates. Compared to conventional methods that consume a substantial amount of chemicals, electrochemical techniques are regarded as green technology (Martínez-Huitle & Panizza 2018).

This is an Open Access article distributed under the terms of the Creative Commons Attribution Licence (CC BY-NC-ND 4.0), which permits copying and redistribution for non-commercial purposes with no derivatives, provided the original work is properly cited (<http://creativecommons.org/licenses/by-nc-nd/4.0/>).

Anodic oxidation technology in particular presents mass transport polarization as the main cell potential inefficiency as it deals with low-concentration pollutants present in wastewater (Nava & Ponce de León 2018). As the relevant reactions require the direct contact between the electrode surface and the pollutant, maximum efficiency is therefore obtained when the electric charge transfer rate and the pollutant's mass transport rate are balanced (Martínez-Huitle *et al.* 2015). The amount of oxidative species generated is regulated by current density, whether the OH radicals are electro-generated at the electrode surface or the oxidizing agents in the bulk (Moreira *et al.* 2017). On the other hand, the targeted substances mass transport is correlated to the hydrodynamic regime (Scialdone 2009). However, the use of deflectors or turbulent promoters at the laboratory scale is not frequently encountered in the literature.

Theoretical modeling provides a reliable representation of the electrochemical oxidation process; it offers a better description of the competition between targeted reactive paths and unwanted reactions. Furthermore, the experimental validation of the mathematical models confirms the modeling assumptions, providing precious insights for the up-scaling phases. Several models therefore have been proposed, particularly in the field of electrochemical treatment of organic pollutants. Comninelis *et al.* proposed a model based on estimation of limiting current, developing a theoretical relationship between instantaneous current efficiency and operative parameters. The model assume mass transfer dependence; thus two behaviors are reported, oxidation control and mass transfer control. They considered the oxidation of water as the only competitive reaction and no homogeneous oxidation processes (Scialdone Galia & Randazzo 2012). Canizares *et al.* proposed an easy-to-use model with no adjustable parameters by representing the reactor as three interconnected stirred-tank reactors. The direct electrochemical process is modeled based on the applied current and the oxidation/reduction potentials of the organic substances involved. The model assumed that the concentration profiles are time dependent and not a function of position. Moreover, at low concentrations, the mass transfer coefficient depends only on flow rate (Cañizares *et al.* 2004). Polcaro *et al.* reported a model describing the evolution of organic concentration; the kinetic model assumes both the direct oxidation of organic substrates adsorbed at the anode surface and the indirect process in the bulk. The model was found to accurately reveal the effect of current density, linear velocity of electrolyte and anode surface to effluent volume ratio on the removal efficiency (Polcaro *et al.* 2002).

In this study, and from an energetic efficiency perspective, CD and SD were of particular interest as their interaction is expected to be significant in anodic oxidation. The limiting step and optimization of CD and SD, in respect to the anodic oxidation of refinery effluent, will be discussed and outlined.

MATERIALS AND METHODS

Materials

The synthetic effluent was prepared the same day the experiments were conducted, and its characteristics were based on Algiers refinery real effluent (Table 1). The characteristics of real wastewater were not the same in various times; a range of variation was reported. To prepare the synthetic effluent within the desired chemical oxygen demand (COD) range, 0.5 mL of toluene was added to each 1,000 mL of distilled water. The effluent was preserved in a water bath at 25 °C (toluene solubility in water at 25 °C is 0.535 g/L). Due to its environmental compatibility, sulfate sodium was added as a supporting electrolyte at 0.05 M. Although adding such chemicals is not of interest at the industrial scale, the possibility of enhancing the real effluent conductivity by a pre-concentration of the desalting stream makes this option worth the investigation (Fil *et al.* 2014; Belkacem *et al.* 2017). The anode material was a commercial lead plate (75 × 25 × 3 mm).

Table 1 | Characteristics of Algiers refinery real effluent and the synthetic wastewater

	Real effluent	Synthetic effluent
Temperature (°C)	25–28	25
pH	6.5	5.5
Conductivity (mS)	3	11.8
COD (mg/L)	500–600	487

Electrochemical reactor and experiments

The experiments were performed in a closed and undivided electrochemical reactor of 750 mL (Figure 1), in a galvanostatic mode and at room temperature (i.e. at $20\text{ }^{\circ}\text{C} \pm 2\text{ }^{\circ}\text{C}$). The reactor was filled with 400 mL of effluent, which is magnetically stirred to ensure mass transfer from and towards the electrode surface. The cell was equipped with lead anode and stainless steel cathode with active area of 15 cm^2 (partially immersed). The electrodes were fixed with an inter-electrode distance of 1 cm and were connected to a direct current power supply (AD-305D, AIDA, China). To determine COD removal, the samples were transferred to a spectrophotometer (Jenway 6305 UV/Vis) at 600 nm. Using standard methods (MA315-DCO-1.1), the COD was measured.

Each experiment used 400 mL of synthetic wastewater and the reaction time was 90 min in all experiments. Current density and stirring degree were the desired parameters to study, and the goal was to quantify their effect and interaction on COD removal and electric energy specific consumption (EESC) with insights on mass transfer coefficient (km).

The responses are computed as follows:

$$\text{COD removal (\%)} = \frac{\text{COD}_0 - \text{COD}_f}{\text{COD}_0} * 100 \quad (1)$$

where COD_0 and COD_f are the initial and final COD values, respectively.

The mass transport coefficient km was estimated by (Equation (2)) (Ibrahim 2013; Muazu *et al.* 2015):

$$km \text{ (cm/s)} = \frac{V_r}{A_e \cdot t} \cdot \ln \frac{\text{COD}_0}{\text{COD}_f} \quad (2)$$

where V_r is the volume of the electrolyte (cm^3), A_e is the active surface area of the electrode (cm^2), t is the reaction time (s), COD_0 and COD_f are the initial and final concentration of the effluent (mg/L).

$$\text{EESC (KWh/kg)} = \frac{U \cdot I \cdot t}{\Delta \text{COD} \cdot V} \quad (3)$$

where U is the cell potential (V), I is the applied current (A), t is the time over which the treatment occurs (s), V is the electrolyte volume (L), ΔCOD is the change in COD value (g/L).

Experimental design and statistical analysis

The experimental design was used to model the COD removal, mass transfer and energy consumption. To assess the relation between current and hydrodynamics, the effect of CD and SD and their interactions were investigated. Table 2 presents the input factors (CD and SD), their dimensions and their values.

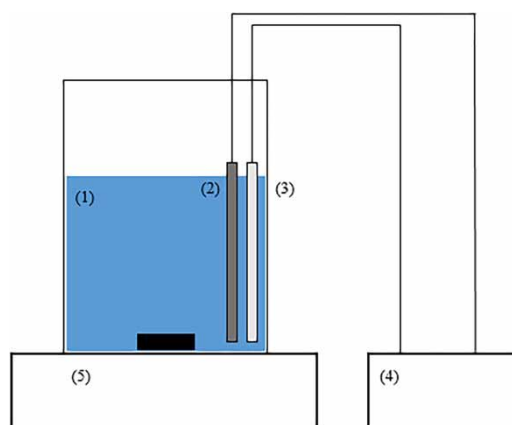


Figure 1 | Schematic diagram of the experimental setup: (1) reactor, (2) anode, (3) cathode, (4) power supply, (5) magnetic stirrer.

Table 2 | Experimental domain and levels of factors

Factors	Unit	Symbol	Study domain		
			Low (-1)	Middle (0)	High (+1)
Current density	mA/cm ²	CD	26.7	30	33.3
Stirring degree	rpm	SD	310	365	420

The study aims to provide insights regarding the contribution of the factors and their interactions to the desired responses. Therefore, a full factorial plan with two central points ($2^k + 2$) was conducted, with a total of six experiments for two factors with two levels. According to the design of experiments (Goupy & Creighton 2006), the following model for the response (Y), as a polynomial equation of independent factors, is presented (Equation (4)):

$$Y = a_0 + \sum a_i x_i + \sum a_{ij} x_i x_j + e \quad (4)$$

where a_0 is a constant number, a_i is the slope of the factor, a_{ij} is a linear interaction between the factors of x_i and x_j . Analysis of variance (ANOVA) was used to examine the significance of each factor (operating parameters). In the ANOVA, the factor significance was defined by Student's t test (T). When the calculated T_i is higher than the T_{cri} in the table, it indicates the significance of the factor. The calculated T_i is obtained by dividing the absolute value of the slope by the square root of common variance of effects as follows:

$$t_i = \frac{\text{Abs}(a_i)}{S_i} \quad (5)$$

The design of experiments included six runs (four runs and two replicates at the central point). Table 3 presents the response values. Experiments were carried out randomly to minimize experimental errors.

RESULTS AND DISCUSSION

Designing experiments and analyzing the variance of responses

Assessing the interaction of factors and quantifying their effect on COD removal, mass transfer coefficient and energy consumption were the aims of this study. Using a full factorial plan, the effect of CD and SD and their interactions were studied to obtain concrete insights about the feasibility of developing a regulation system to optimize current efficiency (CE). Table 3 presents the empirical results of COD removal and the calculated values of mass transfer coefficient and EESC. Using the least standard squares as statistical analysis method, the mathematical model predicted the following responses in terms

Table 3 | Experimental matrix and responses

Run No.	Factors		Responses		
	CD (mA/cm ²)	SD (rpm)	COD removal (%)	km (cm/s)	EESC (KWh/kg)
01	26.7	310	36.35	0.000037	61.01
02	33.3	310	42.51	0.000045	69.75
03	30	365	46.61	0.000052	53.52
04	30	365	50.72	0.000058	49.19
05	26.7	420	52.77	0.000062	39.12
06	33.3	420	50.10	0.000057	57.63

of the factors:

$$\text{COD removal} = 46.51 + 0.8725\text{CD} + 6.0025\text{SD} - 2.2075\text{CD}*\text{SD} \tag{6}$$

$$km = 0.000052 + 0.000001\text{CD} + 0.000009\text{SD} - 0.0000035\text{CD}*\text{SD} \tag{7}$$

$$\text{EESC} = 55.037 + 6.813\text{CD} - 8.503\text{SD} + 2.443\text{CD}*\text{SD} \tag{8}$$

Figure 2 shows the predicted values of the models in comparison with the observed values. These results display a good agreement between predicted and experimental values.

Table 4 presents the results of ANOVA test for coefficients assessment. With a level of confidence of 95% and degrees of freedom $6-4=2$, T_i was compared to the tabulated $T_{\text{cri}} = 4.303$ to assess coefficient significance.

As shown, the calculated T_i for the SD coefficient is significant for the modeled responses ($T_i > T_{\text{cri}}$). However, the binary interaction between the variables was found to be non-significant. Similarly, the test reveals a higher significance effect of CD coefficient on energy consumption compared to the other responses.

Charge rate and mass transfer rate interaction

As mentioned earlier, this study investigated the interaction of current density and stirring degree on COD removal and energy consumption. Figures 3 and 4 illustrate the effects of interaction of factors on responses. Figure 3 shows an interesting interaction between CD and SD. COD abatement experienced a slight decrease when operating at 420 rpm, whereas an increase is observed at the lower level, indicating a negative and positive effect of CD, respectively. Similar trends were reported elsewhere (Ibrahim 2013; Belkacem et al. 2017; Moreira et al. 2017; García-Espinoza & Nacheva 2019). This behavior can be explained by the shift in the limiting step, i.e. the operating regime. An oxidation-controlled process is characterized by higher values of current efficiency and linear decay, whereas mass transport-controlled processes experience exponential abatement and moderate current efficiency values (Kapalka et al. 2008; Scialdone 2009; Muazu et al. 2015). This gives rise to the limiting current concept, which is defined as the threshold at which the charge transfer rate and mass transfer

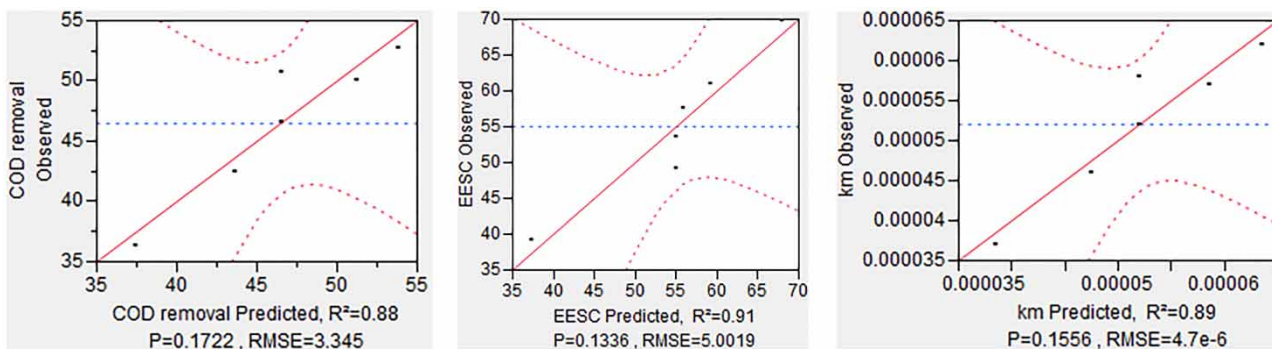


Figure 2 | Compared values of experimental and predicted data of responses.

Table 4 | Analysis of variance (ANOVA) and Student's t test for presented models

Model		COD removal	km	EESC
Variance of residuals (S^2)		11.1890625	2.25×10^{-11}	25.0192292
Variance of common effects (S_i^2)		1.86484375	3.75×10^{-12}	4.16987153
T_i	a_0	34.0584685	26.8526845	26.9519868
	a_1	0.63891666	0.51639778	3.33614699
	a_2	4.39552692	4.64758002	4.1637563
	a_{12}	1.61651406	1.80739223	1.19611582

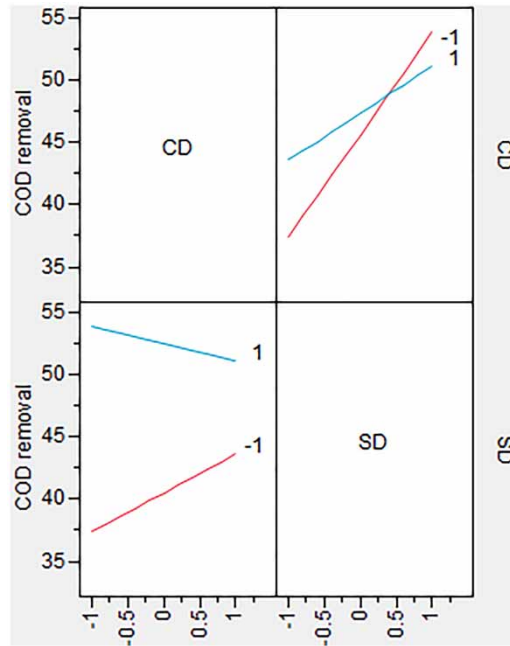


Figure 3 | Effect of interaction of CD and SD on COD removal.

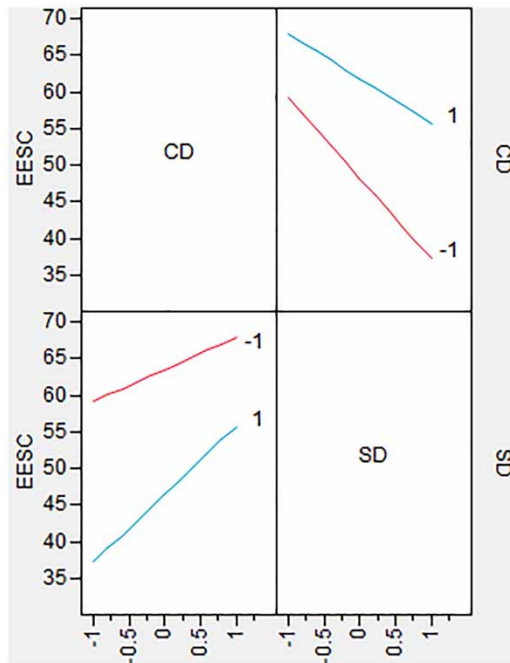


Figure 4 | Effect of interaction of CD and SD on EESC.

rate are balanced (Equation (9)). For a given hydrodynamic regime and initial concentration, degradation efficiency increases with the increase of current until the applied current reaches the limiting value ($I_{app} = I_{lim}$), above which parasite reactions occur (Ghanim 2020).

$$I_{lim} = n \cdot F \cdot km \cdot C_0 \tag{9}$$

On the other hand, Figure 4 indicates a significant decrease in EESC over the SD domain when operating at 26.7 mA/cm², with 10.5 KWh/kg gain for one order of magnitude (55 rpm). Simultaneously, SD has a remarkable effect on COD removal, around 8.2% removal gain, as shown in Figure 3. Although, these responses reflect higher current efficiency when increasing SD and lowering CD, operating at these conditions is not favorable as it slows the reaction kinetics, thus affecting the overall process efficiency. Therefore, balancing the reaction kinetics and the removal efficiency, for a given electrochemical cell, by manipulating the cell hydrodynamics and the applied current is crucial for process optimization (Kapalka *et al.* 2008).

Optimization of operating parameters

The values of the parameters were obtained to maximize the percentage of COD removal and minimize the energy consumption. These optimal values, along with the percentage of COD removal and energy consumption, were computed through the desirability function. A maximum rate of COD removal of 53.85% with a minimum energy consumption of 37.28 KWh/kg was obtained at 26.7 mA/cm² and 420 rpm. These results agree with the interaction diagram's output, which shows that the process efficiency is favorable at turbulent hydrodynamic regimes and lower currents. Therefore, within the studied domain, the process operates above the limiting current; thus, the reaction kinetics is under mass transport control. The gradual degradation of organics eventually leads the process to be mass transport dependent. Operating in batch mode, therefore, requires a regulation system in order to maintain its performance. For a desired COD removal and given cell hydrodynamics, the batch process is optimized by adjusting the current to the limiting value as function of treatment time, more specifically, substrate concentration. The initial limiting current is computed by Equation (9), where mass transfer coefficient can be estimated through a simple current-limiting technique (Scott & Lobato 2002). The theoretical temporal evolution of the limiting current is then given by Equation (10). Furthermore, to achieve a desired COD removal, the electrolysis time τ is estimated through Equation (11), where τc is the time constant of the cell (Equation (12)) (Kapalka *et al.* 2008).

$$i_{lim} = i_{lim0} \cdot \exp\left(-\frac{t}{\tau c}\right) \quad (10)$$

$$\tau = -\tau c \cdot \text{Log} \frac{COD_f}{COD_0} \quad (11)$$

$$\tau c = \frac{Vr}{A \cdot km} \quad (12)$$

From an energy efficiency perspective, and for comparison's sake, reporting the characteristics of the electrochemical cell in details is crucial, since the mass transport coefficient is correlated to both flow rate and cell design. Alongside the conventional parameters reported in the major studies, concrete insights about the limitations of an adapted treatment are then accessible. Reporting these data in future studies is expected to significantly contribute to the electrochemical cell design adaptation towards large-scale applications.

Mass transport and process performance

As poor hydrodynamic conditions can affect substantially the action of the current density, monitoring species mass transfer coefficient is of high interest. In addition to mass transfer enhancement, proper hydrodynamics contribute to the overall process efficiency, through the applied shear stresses, by lowering the film layer thickness at the catalytic surface (Fil *et al.* 2014), thus reducing the effect of electrode poisoning. Figure 5 shows the plot of COD removal, EESC and km in term of CD and SD. Mass transfer coefficient was found to be inversely correlated to EESC. Beyond the studied domain, it was found that around 62% COD removal can be achieved at 26.7 mA/cm² (−1) and 475 rpm (2), with only 26 KWh/kg. It is explained by enhancing the rate at which targeted contaminants collide with the electrode surface, which leads to favoring the desired reactions. However, this effect occurs up to a threshold above which no significant change is observed. At this point, the process is under current limitation and further removals require higher current values. Species concentration is another factor that is found to affect this balance. Trends where degradation efficiency is higher at early stages were reported (Ibrahim 2013; Jawad & Abbar 2019).

The applied current values and cell hydrodynamics give rise to different operating regimes. Mass transport control occurs when, for a given substrate concentration, the mass transfer rate of the reagent to the anode surface is significantly lower than its oxidation rate ($I_{app} > I_{lim}$). By definition, the instantaneous current efficiency is the ratio of the amount of charge

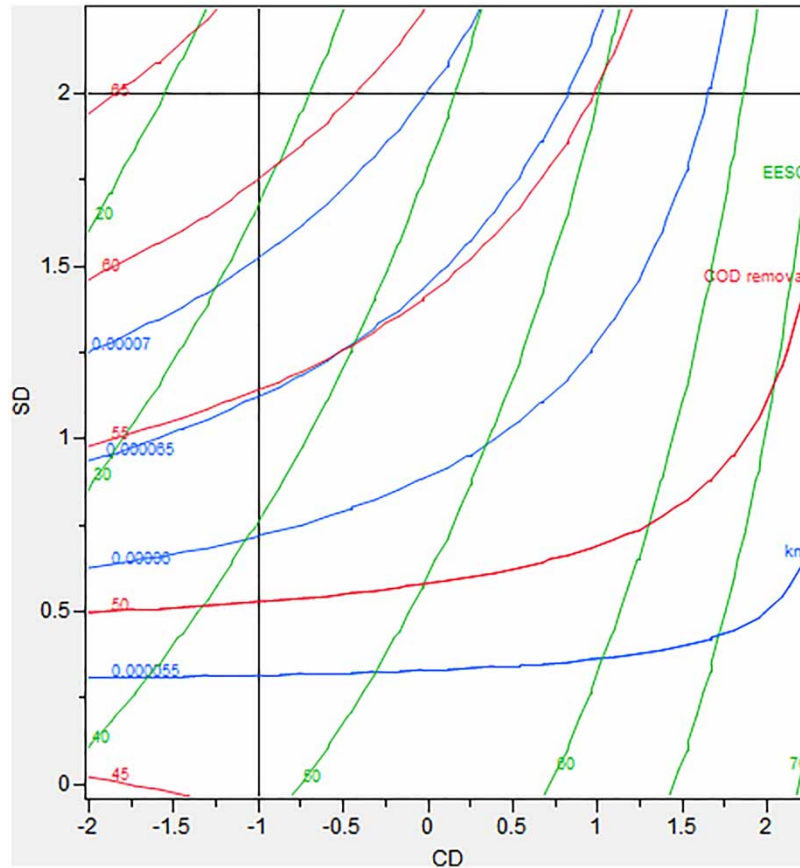


Figure 5 | Iso-response plot, response variation as a function of factors.

delivered to the desired reaction to the total charge (Equation (13)). At the assumption of oxidation reaction occurs only at the anode surface, and water oxidation is the only competitive reaction, the instantaneous current efficiency (ICE) is given by the ratio between I_{lim} and applied current (Equation (14)) (Scialdone 2009) and its temporal evolution by (Equation (15)) (Kapalka *et al.* 2008) where $\alpha = i/i_{lim}^0$.

$$ICE = -\frac{n.F.V.dC}{dQ} \quad (13)$$

$$ICE^{MT} = \frac{n.F.km.C}{i_{app}} \quad (14)$$

$$ICE^{MT}(t) = \exp\left(\frac{1-\alpha}{\alpha} - \frac{A.km.t}{V_r}\right) \quad (15)$$

It can be seen that current efficiency is a function of applied current, hydrodynamic regime (as it influences the mass transfer coefficient) and the substrate concentration (with a linear dependence). Interestingly, the current efficiency is independent of the reaction mechanisms when operating under mass transport control.

Contrastingly, oxidation control occurs at lower current values, when the rate at which organic substrate arrives at the anode surface is dramatically higher than its oxidation rate ($I_{app} \ll I_{lim}$). Considering both direct and indirect oxidation routes, the instantaneous current efficiency is expressed by Equation (16). Where C^* is the value of C_0 , which gives a current density for the substrate oxidation equal to the current density involved for the oxygen evolution reaction, it depends on the oxidation path (Cominellis 1994; Scialdone 2009). Hence, under oxidation reaction control, the ICE depends only on the

substrate concentration and the oxidation route.

$$ICE^{OC} = \frac{1}{1 + \frac{C^*}{C_b}} \quad (16)$$

As electrochemical technologies deal with low-concentration effluents, it is clear that mass transport enhancement in continuous reactors is vital to the up-scaling of this technology.

CONCLUSION

In this study, the relation between current density and stirring degree in anodic oxidation of synthetic wastewater was investigated. A full factorial plan was used to design experiments. The effects of the factors and their interactions on COD removal, EESC and mass transport were quantified and the results were analyzed using ANOVA. It was found that the stirring degree was significant and effective on all responses within the studied domain. A 55 rpm variation in stirring degree was found to affect COD removal and EESC by a gain of 6% and 8.5 KWh/kg, respectively. The highest COD removal and minimum energy consumption obtained by the presented model, computed through the desirability function, were 53.85% and 37.28 KWh/kg at 420 rpm and 26.7 mA/cm².

Beyond reporting trends, the balance between charge rate and mass transport rate was emphasized, as it offers precious insights on how to align cell design and regulation with proper feeds. Reporting similar data in future studies will conveniently reflect the system limitations and, eventually, allow concrete adjustments towards large applications. Finally, the necessity of considering new comparative concepts was discussed.

DATA AVAILABILITY STATEMENT

All relevant data are included in the paper or its Supplementary Information.

REFERENCES

- Ali, D., al deen, A., Palaniandy, P. & Feroz, S. 2018 *Advanced Oxidation Processes (AOPs) to Treat the Petroleum Wastewater*. <https://doi.org/10.4018/978-1-5225-5766-1.ch005>.
- Aljoubury, D. A. D. A., Palaniandy, P., Abdul Aziz, H. B. & Feroz, S. 2017 *Treatment of petroleum wastewater by conventional and new technologies – a review*. *Global Nest Journal* **19**, 439–452. <https://doi.org/10.30955/gnj.002239>.
- Al-Khalid, T. & El-Naas, M. H. 2018 *Organic contaminants in refinery wastewater: characterization and novel approaches for biotreatment*. *Recent Insights in Petroleum Science and Engineering*. <https://doi.org/10.5772/intechopen.72206>.
- Bartolomeu, M., Neves, M. G. P. M. S., Faustino, M. A. F. & Almeida, A. 2018 *Wastewater chemical contaminants: remediation by advanced oxidation processes*. *Photochemical and Photobiological Sciences* **17**, 1573–1598. <https://doi.org/10.1039/c8pp00249e>.
- Belkacem, S., Bouafia, S. & Chabani, M. 2017 *Study of oxytetracycline degradation by means of anodic oxidation process using platinized titanium (Ti/Pt) anode and modeling by artificial neural networks*. *Process Safety and Environmental Protection* **111**, 170–179. <https://doi.org/10.1016/j.psep.2017.07.007>.
- Cañizares, P., García-Gómez, J., Lobato, J. & Rodrigo, M. A. 2004 *Modeling of wastewater electro-oxidation processes part I. general description and application to inactive electrodes*. *Industrial and Engineering Chemistry Research* **43** (9), 1915–1922. <https://doi.org/10.1021/ie0341294>.
- Comninellis, C. 1994 *Electrocatalysis in the electrochemical conversion/combustion of organic pollutants for waste water treatment*. *Electrochimica Acta* **39** (11–12), 1857–1862. [https://doi.org/10.1016/0013-4686\(94\)85175-1](https://doi.org/10.1016/0013-4686(94)85175-1).
- Fakhru'l-Razi, A., Pendashteh, A., Abdullah, L. C., Biak, D. R. A., Madaeni, S. S. & Abidin, Z. Z. 2009 *Review of technologies for oil and gas produced water treatment*. *Journal of Hazardous Materials* **170**, 530–551. <https://doi.org/10.1016/j.jhazmat.2009.05.044>.
- Fil, B. A., Boncukcuoğlu, R., Yilmaz, A. E. & Bayar, S. 2014 *Electro-oxidation of pistachio processing industry wastewater using graphite anode*. *CLEAN – Soil, Air, Water* **42** (9), 1232–1238. <https://doi.org/10.1002/clen.201300560>.
- García-Espinoza, J. D. & Nacheva, P. M. 2019 *Degradation of pharmaceutical compounds in water by oxygenated electrochemical oxidation: parametric optimization, kinetic studies and toxicity assessment*. *Science of the Total Environment* **691**, 417–429. <https://doi.org/10.1016/j.scitotenv.2019.07.118>.
- Ghanim, A. N. 2020 *Perspectives of electrochemical oxidation parameters in PRW treatment*. *International Journal of Environment and Waste Management* **26** (3), 349–361. <https://doi.org/10.1504/IJEWM.2020.109166>.
- Goupy, J. & Creighton, L. 2006 *Introduction aux plans d'expériences*, 3rd edn. Dunod, Paris.
- Ibrahim, D. S. 2013 *Electrochemical oxidation treatment of petroleum refinery effluent*. *International Journal of Scientific & Engineering Research* **4** (8), 0–5. <https://doi.org/10.14299/00000>.

- Jawad, S. S. & Abbar, A. H. 2019 Treatment of petroleum refinery wastewater by electrochemical oxidation using graphite anodes. *Al-Qadisiyah Journal for Engineering Sciences* **12** (3), 144–150. <https://doi.org/10.30772/qjes.v12i3.609>.
- Kapalka, A., Fóti, G. & Comninellis, C. 2008 Kinetic modelling of the electrochemical mineralization of organic pollutants for wastewater treatment. *Journal of Applied Electrochemistry* **38** (1), 7–16. <https://doi.org/10.1007/s10800-007-9365-6>.
- Martínez-Huitle, C. A. & Panizza, M. 2018 Electrochemical oxidation of organic pollutants for wastewater treatment. *Current Opinion in Electrochemistry* **11**, 62–71. <https://doi.org/10.1016/j.coelec.2018.07.010>.
- Martínez-Huitle, C. A., Rodrigo, M. A., Sirés, I. & Scialdone, O. 2015 Single and coupled electrochemical processes and reactors for the abatement of organic water pollutants: a critical review. *Chemical Reviews* **115**, 13362–13407. <https://doi.org/10.1021/acs.chemrev.5b00361>.
- Moreira, F. C., Boaventura, R. A. R., Brillas, E. & Vilar, V. J. P. 2017 Electrochemical advanced oxidation processes: a review on their application to synthetic and real wastewaters. *Applied Catalysis B: Environmental* **202**, 217–261. <https://doi.org/10.1016/j.apcatb.2016.08.037>.
- Muazu, N. D., Jarrah, N. & Bukhari, A. 2015 Kinetic modeling of electrochemical oxidation of phenol on boron-doped diamond anode in the presence of some inorganic species. *Desalination and Water Treatment* **56** (11), 3005–3012. <https://doi.org/10.1080/19443994.2014.964329>.
- Nava, J. L. & Ponce de León, C. 2018 Reactor design for advanced oxidation processes. In: Zhou, M., Oturan, M. & Sirés, I. (eds), *Electro-Fenton Process. The Handbook of Environmental Chemistry*, Vol. 61, Springer, Singapore, pp. 263–286. https://doi.org/10.1007/978-94-007-698-2_54.
- Polcaro, A. M., Mascia, M., Palmas, S. & Vacca, A. 2002 Kinetic study on the removal of organic pollutants by an electrochemical oxidation process. *Industrial and Engineering Chemistry Research* **41** (12), 2874–2881. <https://doi.org/10.1021/ie010669u>.
- Scialdone, O. 2009 Electrochemical oxidation of organic pollutants in water at metal oxide electrodes: a simple theoretical model including direct and indirect oxidation processes at the anodic surface. *Electrochimica Acta* **54** (26), 6140–6147. <https://doi.org/10.1016/j.electacta.2009.05.066>.
- Scialdone, O., Galia, A. & Randazzo, S. 2012 Electrochemical treatment of aqueous solutions containing one or many organic pollutants at boron doped diamond anodes. Theoretical modeling and experimental data. *Chemical Engineering Journal* **183**, 124–134. <https://doi.org/10.1016/j.cej.2011.12.042>.
- Scott, K. & Lobato, J. 2002 Determination of a mass-transfer coefficient using the limiting-current technique. *The Chemical Educator* **7** (4), 214–219. <https://doi.org/10.1007/s00897020579a>.
- Singh, S. & Shikha, J. 2019 Treatment and Recycling of Wastewater From Oil Refinery/Petroleum Industry. In: Singh, R. & Singh, R. (eds) *Advances in Biological Treatment of Industrial Waste Water and Their Recycling for a Sustainable Future. Applied Environmental Science and Engineering for a Sustainable Future*. Springer, Singapore. https://doi.org/10.1007/978-981-13-1468-1_10.
- Yan, L., Wang, Y., Li, J., Ma, H., Liu, H., Li, T. & Zhang, Y. 2014 Comparative study of different electrochemical methods for petroleum refinery wastewater treatment. *Desalination* **341** (1), 87–93. <https://doi.org/10.1016/j.desal.2014.02.037>.

First received 17 June 2021; accepted in revised form 13 September 2021. Available online 27 September 2021